AIP | Physics of Plasmas

Simulation of non-resonant internal kink mode with toroidal rotation in the National Spherical Torus Experiment

Feng Wang, G. Y. Fu, J. A. Breslau, Kevin Tritz, and J. Y. Liu

Citation: Phys. Plasmas **20**, 072506 (2013); doi: 10.1063/1.4816026
View online: http://dx.doi.org/10.1063/1.4816026
View Table of Contents: http://pop.aip.org/resource/1/PHPAEN/v20/i7
Published by the AIP Publishing LLC.

Additional information on Phys. Plasmas

Journal Homepage: http://pop.aip.org/
Journal Information: http://pop.aip.org/about/about_the_journal
Top downloads: http://pop.aip.org/features/most_downloaded
Information for Authors: http://pop.aip.org/authors

ADVERTISEMENT

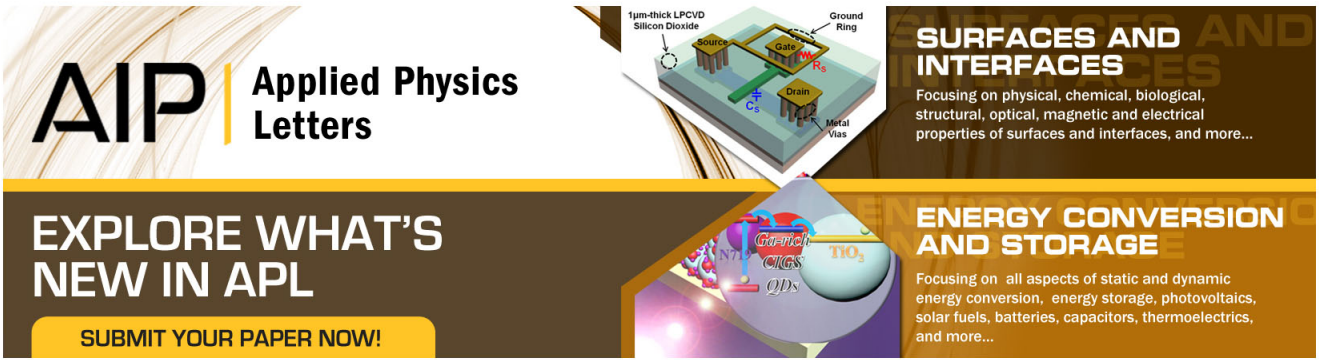

Downloaded 04 Sep 2013 to 198.125.229.230. This article is copyrighted as indicated in the abstract. Reuse of AIP content is subject to the terms at: http://pop.aip.org/about/rights_and_permissions

Simulation of non-resonant internal kink mode with toroidal rotation in the National Spherical Torus Experiment

Feng Wang,[1] G. Y. Fu,[2,a)] J. A. Breslau,[2] Kevin Tritz,[3] and J. Y. Liu[1,b)]
[1]*School of Physics and Optoelectronic Technology, Dalian University of Technology, Dalian 116024, China*
[2]*Princeton Plasma Physics Laboratory, Princeton, New Jersey 08543, USA*
[3]*Department of Physics and Astronomy, Johns Hopkins University, Baltimore, Maryland 21218, USA*

(Received 22 April 2013; accepted 18 June 2013; published online 25 July 2013)

Plasmas in spherical and conventional tokamaks, with weakly reversed shear q profile and minimum q above but close to unity, are susceptible to an non-resonant $(m,n) = (1,1)$ internal kink mode. This mode can saturate and persist and can induce a (2,1) seed island for Neoclassical Tearing Mode. [Breslau *et al*. Nucl. Fusion **51**, 063027 (2011)]. The mode can also lead to large energetic particle transport and significant broadening of beam-driven current. Motivated by these important effects, we have carried out extensive nonlinear simulations of the mode with finite toroidal rotation using parameters and profiles of an NTSX plasma with a weakly reversed shear profile. The numerical results show that, at the experimental level, plasma rotation has little effect on either equilibrium or linear stability. However, rotation can significantly influence the nonlinear dynamics of the (1,1) mode and the induced (2,1) magnetic island. The simulation results show that a rotating helical equilibrium is formed and maintained in the nonlinear phase at finite plasma rotation. In contrast, for non-rotating cases, the nonlinear evolution exhibits dynamic oscillations between a quasi-2D state and a helical state. Furthermore, the effects of rotation are found to greatly suppress the (2,1) magnetic island even at a low level. © *2013 AIP Publishing LLC*. [http://dx.doi.org/10.1063/1.4816026]

I. INTRODUCTION

In spherical tokamaks like the National Spherical Torus Experiment (NSTX) or the Mega-Ampere Spherical Tokamak (MAST), high β plasmas with weakly reversed q profiles and minimum safety factor q_{min} close to but greater than unity are susceptible to an global ideal MHD instability called the non-resonant internal kink mode (NRK), as predicted by Hastie *et al*.[2] Recent stability calculations of NRK in spherical tokamaks have confirmed this prediction.[1,3,4] This mode, which is related to the infernal mode,[5] was used successfully to explain the Long Lived Mode (LLM) observed in MAST.[3,4] Recent nonlinear simulations by Breslau *et al*.[1] showed that the n = 1 NRK can be unstable in NSTX plasmas with weakly reversed q profile when q_{min} is sufficiently close to unity, and that it can nonlinearly saturate and induce a (2,1) magnetic island at the $q = 2$ surface. This induced (2,1) island could explain the triggerless (2,1) Neoclassical Tearing Mode (NTM) observed in such NSTX plasmas.[6] This mode can also lead to large fast ion transport and broadening of beam-driven current resulting in significant modification of the q profile.[3,7,8] Furthermore, NRK has important implications for the advanced operation regime of conventional tokamaks, where similar saturated kink modes or long lived modes have been observed.

Following the previous work by Breslau *et al*.,[1] linear and nonlinear simulations of the NRK have been carried out for an NSTX plasma using the extended MHD code M3D.[9] Our work extends the previous work[1,3,4] by retaining finite toroidal rotation. Our simulation results show nearly steady state saturation of the NRK with rotation, similar to the previous result for non-rotating plasmas. More importantly, our results show that the induced (2,1) island is greatly suppressed by effects of toroidal rotation. This result is consistent with the experimental observation of an increased threshold for NTM due to sheared rotation in NSTX.[6]

The rest of this paper is organized as follows. In Sec. II, the simulation model and parameters are briefly described. In Sec. III, results of linear simulations are presented. In Sec. IV, nonlinear simulations are described. Finally, Sec. V gives discussions of this work and conclusions.

II. SIMULATION MODEL, PARAMETERS, PROFILES, AND EQUILIBRIUM SET UP

For this study, the 3D nonlinear extended MHD code M3D (Ref. 9) is used. In particular, we used the dissipative MHD model to simulate the kink mode nonlinearly. The model consists of the full resistive MHD equations plus additional dissipative terms including viscosity and heat conduction.[9] In addition, we used an artificial sound wave method to model fast thermal equilibration along field lines. In this method, a pair of wave equations for the temperature are solved along field lines with wave speed a few times the Alfvén speed (see Eqs. (8) and (9) in Ref. 9). This method was found to improve the accuracy of the parallel temperature equilibration over that of the standard parallel heat diffusion equation used in the previous work.[1] In the M3D code, this system of dissipative MHD equations is discretized using linear finite elements on triangular mesh in each poloidal plane and solved as an initial-value problem.

a)Electronic mail: fu@pppl.gov
b)Electronic mail: jyliu@dlut.edu.cn

 © 2013 AIP Publishing LLC

Downloaded 04 Sep 2013 to 198.125.229.230. This article is copyrighted as indicated in the abstract. Reuse of AIP content is subject to the terms at: http://pop.aip.org/about/rights_and_permissions

As in the previous work,[1] we consider parameters and profiles based on an NBI-heated NSTX plasma (shot #124379 at $t = 0.635$ s) with a weakly reversed shear q profile. The parameters are: major radius $R = 0.858$ m, minor radius $a = 0.602$ m, inverse aspect ratio $\epsilon \equiv a/R = 0.701$, toroidal magnetic field $B_0 = 0.44$ T, density $\rho_0 \equiv n_0 m_i = 3.1 \times 10^{-8}\,\mathrm{kg/m^{-3}}$, Alfvén speed $v_A \equiv \frac{B_0}{(\rho_0 \mu_0)^{1/2}} = 7.07 \times 10^5$ m/s, and Alfvén time $\tau_A = R/v_A$. The normalized pressure profile, q profile and electron density profile are shown in Fig. 1 as a function of the minor radius $r = \sqrt{\Phi}$ with Φ being the normalized toroidal flux. The q profile is nearly flat with minimum of q, $q_{min} = 1.07$, located at $r/a = 0.3$. These profiles were obtained from equilibrium reconstruction and the transport analysis code TRANSP using measured plasma profiles of density, temperature, magnetic field line pitch, and equilibrium toroidal rotation. For most of simulations presented, the value of q_{min} was chosen to be $q_{min} = 1.07$, which is presumed to be within the uncertainty of q profile from equilibrium reconstruction. A resistivity profile took the form $\eta(T) = \eta_0 (T/T_0)^{-3/2}$, where T_0 and η_0 are the temperature and resistivity on axis, respectively. In our simulation, η_0 was set to 5×10^{-6} with corresponding Lundquist number $S = 1/\eta_0 = 2 \times 10^5$. Viscosity was chosen to be 10^{-4} in the plasma core and larger in the edge region. The perpendicular thermal conductivity was $\chi_\perp = 5 \times 10^{-5}$. Radial resolution was 121 radial by 480 poloidal by 12 toroidal zones, and toroidal mode numbers up to $n = 3$ were kept. Time step was $0.01\tau_A$. We have performed a systematic convergence study varying the spactial resolution as well as time step size. We find that the numerical resolution used is adequate for the results to be shown below.

Based on these profiles and parameters, a static equilibrium was calculated using the equilibrium code VMEC based on given pressure and q profiles. The computed equilibrium solution was then used as initial condition for M3D code. For cases with sheared toroidal rotation, M3D itself is used to compute a self-consistent equilibrium by evolving the MHD equations nonlinearly to a steady state using a large viscosity (10^{-3}) and a low resistivity (10^{-6}). And to keep temperature as a flux function, the coefficient of specific heat is set to $\gamma = 1$. After a steady state is reached, the viscosity is turned down to a smaller value on order of 10^{-4} and an initial perturbation is applied to simulate the linear and nonlinear phase. The obtained steady state solution corresponds to a new rotating equilibrium consistent with a prescribed rotation profile. Figure 2 shows that the density profile with toroidal rotation (in red) at twice the experimental level is shifted outward relative to the non-rotating density profile (in black). This rotation-induced shift agrees well with the following analytic model:[10] temperature (T) and toroidal angular velocity (Ω) are both assumed to be poloidal flux functions, $T = T(\psi), \Omega = \Omega(\psi)$, and the density profile is shifted outward,

$$\rho = \rho_0(\psi) e^{(R^2 - R_0^2)\Lambda(\psi)}, \tag{1}$$

where ρ is plasma mass density profile with rotation, R is major radius with R_0 being R at magnetic axis, $\Lambda = \Omega^2/(2T)$.

III. LINEAR STABILITY

We first describe linear simulation results without rotation. Linear calculations of $n = 1$, $n = 2$, and $n = 3$ were performed with the M3D code. The results show that the $n = 1$ mode is unstable with growth rate $\gamma\tau_A = 0.0395$ while both the $n = 2$ and $n = 3$ mode are stable. Here $\tau_A \equiv 1/\omega_A$, $\omega_A = v_A(0)/R_0$, is the toroidal Alfvén transit time. Additional simulations show that $n = 4$ and $n = 5$ modes are also stable. Furthermore, the $n = 1$ growth rate is

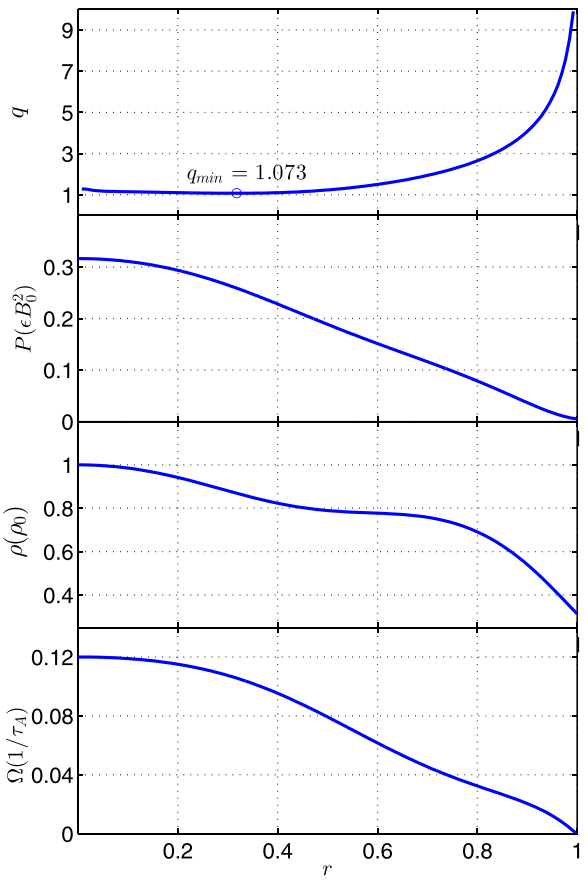

FIG. 1. Equilibrium profile of q, pressure, density (ρ), and toroidal rotation (Ω).

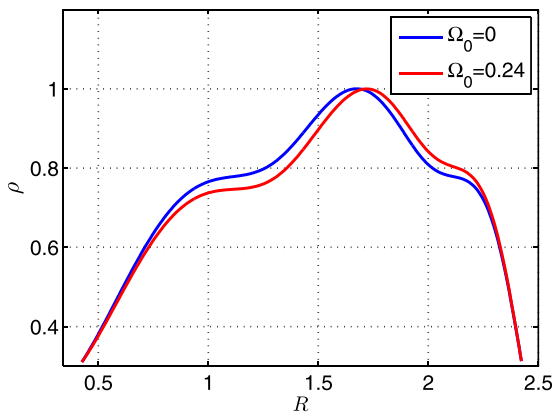

FIG. 2. Density profile with (red) and without rotation.

Downloaded 04 Sep 2013 to 198.125.229.230. This article is copyrighted as indicated in the abstract. Reuse of AIP content is subject to the terms at: http://pop.aip.org/about/rights_and_permissions

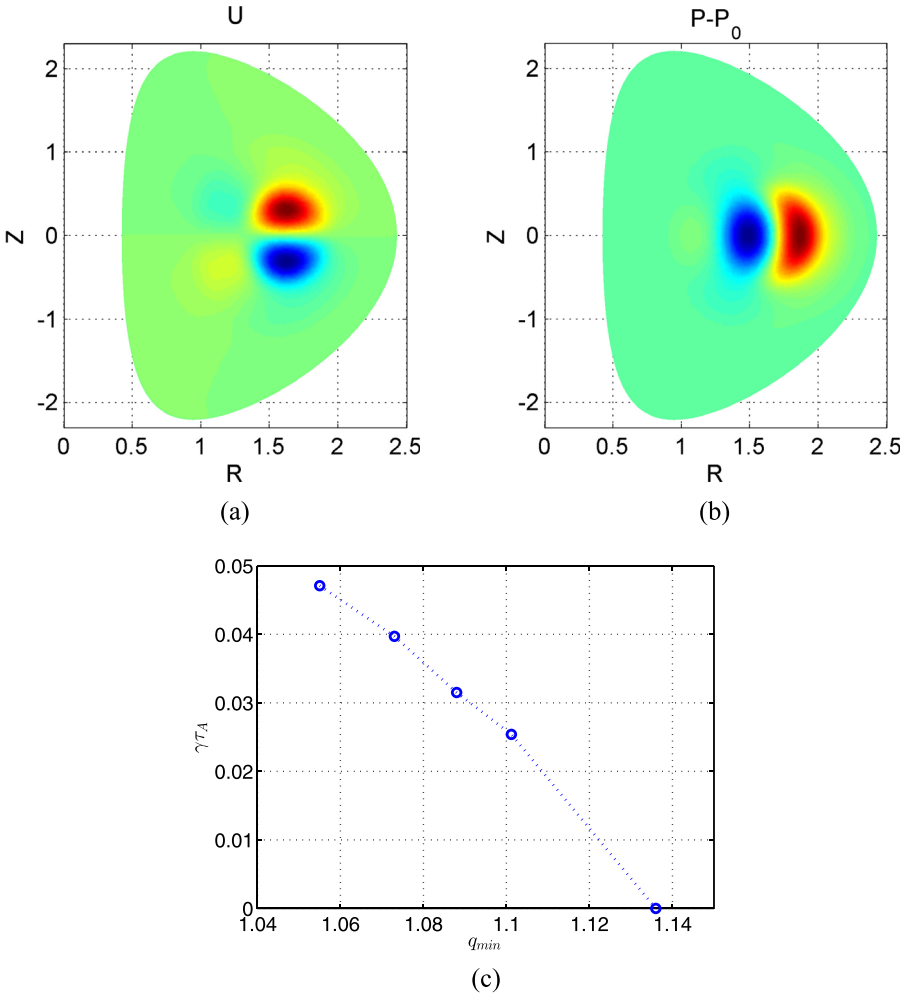

FIG. 3. (a) Linear eigenmode structure of velocity stream function U, (b) pressure perturbation, and (c) growth rate of the $n=1$ NRK versus q_{min}.

almost independent of resistivity for η up to $\eta = 1 \cdot 10^{-4}$, indicating it is an ideal mode. Figures 3(a) and 3(b) show the linear eigenmode structure of the stream function U and the perturbed pressure, where U is related to the incompressible part of the plasma velocity by the following equation:

$$v = R^2 \epsilon \nabla_\perp U \times \nabla\varphi + \nabla\chi + v_\varphi \nabla\phi. \tag{2}$$

We observe that the mode structures are located in the core region and are dominated by the (1,1) harmonic. The mode's stability is found to be very sensitive to the q_{min} value as shown in Fig. 3(c). These linear results are consistent with previous analytic and numerical results.[1–3]

We next consider linear stability in the presence of sheared rotation. In our simulations, the rotation profile from the NSTX experiment is used as shown in Fig. 1. The peak rotation at the magnetic axis is $\Omega_0/\omega_A = 0.12$ which corresponds to $f_0 \simeq 15\,\mathrm{KHz}$ and $v_{\phi,0} \simeq 1 \times 10^5\,\mathrm{m/s}$. It should be noted that this rotational speed is close to the thermal ion speed $v_{th} \simeq 1.8 \times 10^5 \mathrm{m/s}$ for typical NSTX parameters and the rotation is in the same direction as the plasma current.

We have carried out linear simulations of the $n=1$ mode with different rotation speeds. Results in Fig. 4 show that rotation is mostly stabilizing for moderate rotation level, although it is interesting to note that the effect of rotation is actually marginally destabilizing for small rotation values. The stabilizing effect is quite weak at the experimental rotation level (i.e., $\Omega_0/\omega_A = 0.12$). This result is similar to previous stability results.[3,11]

IV. NONLINEAR SIMULATIONS

In this section, we consider the nonlinear evolution of the $n=1$ NRK in the NSTX plasma with and without rotation. Below, we first present results without rotation.

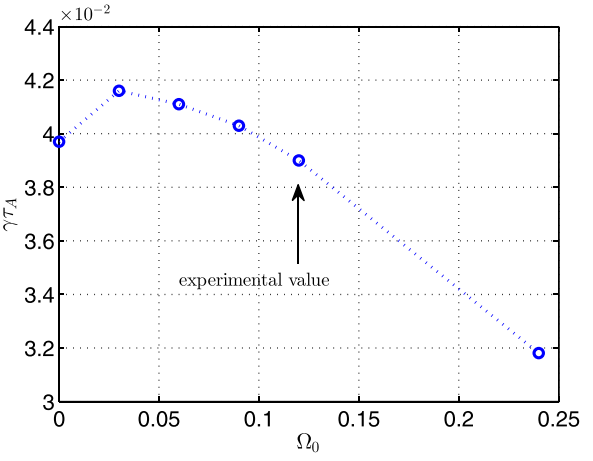

FIG. 4. The $n=1$ linear growth rate versus rotation frequency.

Downloaded 04 Sep 2013 to 198.125.229.230. This article is copyrighted as indicated in the abstract. Reuse of AIP content is subject to the terms at: http://pop.aip.org/about/rights_and_permissions

A. Nonlinear dynamics without toroidal rotation

In nonlinear simulations with M3D, current and pressure sources are used and held fixed in time. These sources are prescribed to be consistent with the corresponding pressure and current profiles, i.e., the equilibrium is at steady state in 2D. Figure 5(a) shows the kinetic energy evolution for toroidal mode numbers $n = 0$, 1, 2, 3. In the initial linear phase, the $n = 1$ mode grows with growth rate $\gamma\tau_A = 0.0395$. After this linear phase, the high-n components are driven unstable nonlinearly with $\gamma_{n=2} \simeq 2\gamma_{n=1}$ and $\gamma_{n=3} \simeq 3\gamma_{n=1}$. After a short time of nonlinear growth, the modes saturate at about $t = 300\tau_A$. In this early nonlinear phase, an $m/n = 2/1$ magnetic island begins to emerge as shown in Fig. 5(b). This island is induced nonlinearly by the main (1,1) mode. After the (1,1) mode is saturated, the (2,1) island still keeps growing for a short time before reaching a quasi-steady state [Fig. 5(c)]. It has been suggested that this induced island can act as a trigger for the NTM mode observed in the NSTX plasma.[1]

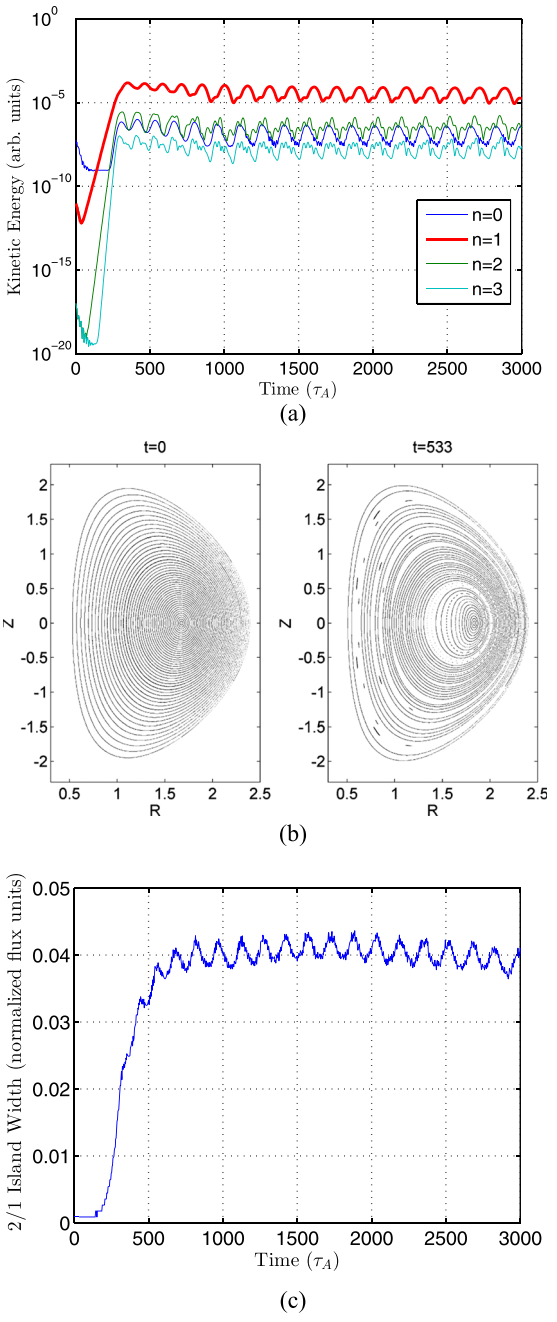

FIG. 5. (a) Kinetic energy evolution of toroidal mode numbers $n = 0$, 1, 2, and 3; (b) Poincare plot at *time* $= 0\tau_A$ (left) and *time* $= 533\tau_A$ (right); (c) evolution of $m/n = 2/1$ island width.

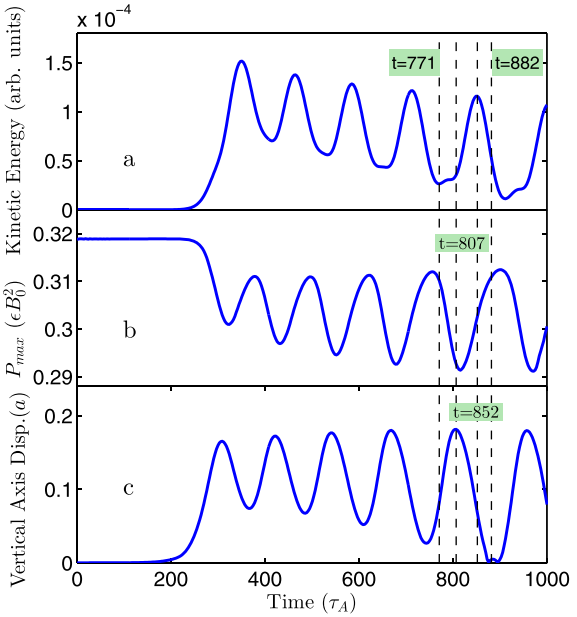

FIG. 6. Nonlinear evolution of (a) $n = 1$ component kinetic energy, (b) maximum of pressure, and (c) vertical axis displacement.

It is interesting to note that, after the initial saturation of the $n = 1$ energy, a quasi-periodic nonlinear oscillative phase emerges with a period around $t_{period} \simeq 120$. Fig. 6 shows the relative phase of oscillations in mode kinetic energy, peak pressure value, and magnetic axis shift and Fig. 7 shows the corresponding evolution of Poincare contours of magnetic

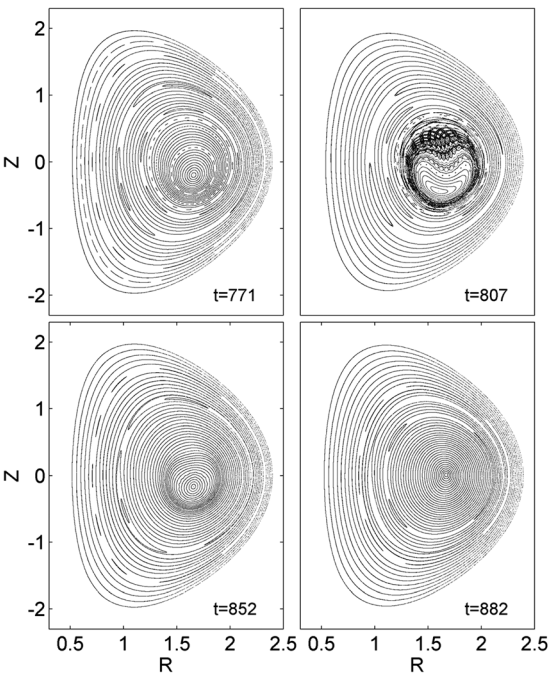

FIG. 7. Evolution of Poincare magnetic field topology during an oscillation period.

Downloaded 04 Sep 2013 to 198.125.229.230. This article is copyrighted as indicated in the abstract. Reuse of AIP content is subject to the terms at: http://pop.aip.org/about/rights_and_permissions

field lines during a representative period (from $t = 771$ to $t = 882$). It is clear that the peak pressure evolution is out of phase with the magnetic axis shift. However, there is roughly 90° phase shift between the mode kinetic energy oscillation and axis shift, We also note that at $t = 882$, at the minimum of axis shift, the magnetic flux surfaces recover roughly the 2D axi-symmetric state except the remaining (2,1) island. The details of the physical mechanism for this nonlinear oscillation will be examined in future. Finally, it is important to note that during these large oscillation of magnetic configurations and the mode energy, the (2,1) island width remains roughly constant with correspondingly small-amplitude oscillations.

It should be pointed out that, although our results here (at zero rotation) are similar to those of previous results,[1] there is one important difference. Our results indicate that the mode saturation is dynamic with large oscillations in mode energy and magnetic configuration, whereas the previous results gave steady state saturation corresponding to a helical equilibrium. The difference is mainly due to the different parameters used and the different models for the parallel heat conduction. In this work, we used a smaller viscosity ($\mu = 10^{-4}$) and the artificial sound wave method for parallel heat conduction. We have carried out a systematic study of the dependence of the oscillation on dissipation parameters and the parallel heat conduction model. We find that the nonlinear oscillations are suppressed by using larger values of viscosity (i.e., $\mu \sim 3 \times 10^{-4}$) or by turning off the artificial sound wave method. In Sec. IV B, we will show that a finite toroidal rotation can also suppress these dynamic oscillations.

B. Nonlinear saturation with toroidal rotation

We now present the first nonlinear simulation results of NRK with finite toroidal rotation. In our simulations, the full effects of plasma toroidal rotation are retained with a rotation source consistent with the initial rotating equilibrium. Figure 8(a) shows a comparison of kinetic energy evolution between rotating and non-rotating cases using the experimental profile (both shape and value). We observe that the mode kinetic energy evolution is almost the same in the linear and early nonlinear phase in the two cases. However, there is a striking difference in the nonlinear phase after the initial mode saturation, namely, the large nonlinear oscillations in the non-rotating case are suppressed in the rotating case, where a steady state saturation is now reached. Figure 8(b) shows the corresponding evolution of the magnetic axis shift. It is clear that, in the rotating case, a steady state helical equilibrium is established and maintained and is rotating at the frequency close to the core rotation frequency of $f_{rotation,0} \simeq 15\,\mathrm{KHz}$. We have carried out a study of the dependence of nonlinear saturation on the level of plasma rotation. Figure 9 shows the mode kinetic energy evolution at three rotation levels. We observe that the nonlinear oscillation can be suppressed for rotation value as low as $\Omega_0/\omega_A = 0.06$, which is half of the NSTX value.

A more important effect of plasma rotation is its suppression of the (2,1) magnetic island. Figure 10 shows the

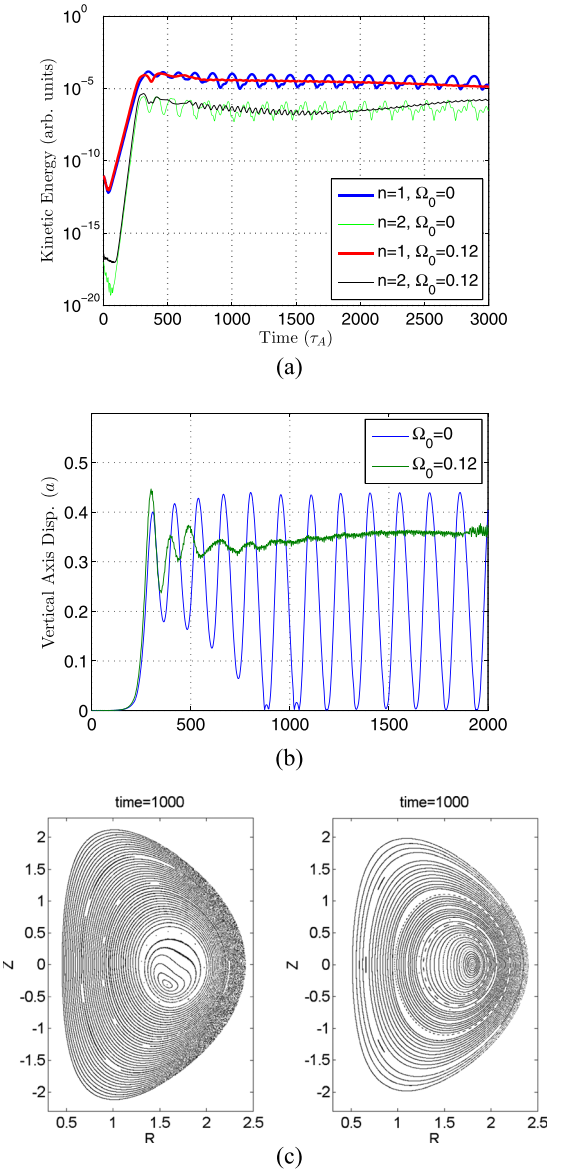

FIG. 8. (a) Evolution of the $n = 1$ and $n = 2$ kinetic energy with and without rotation; (b) evolution of magnetic axis shift with (green) and without (blue) rotation; (c) Poincare plot without rotation; (d) Poincare plot with rotation.

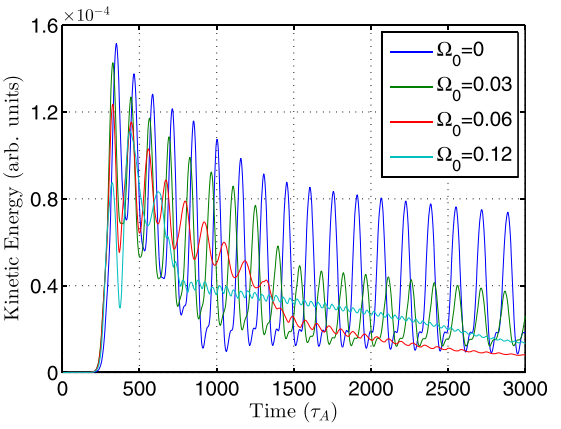

FIG. 9. Nonlinear evolution of total kinetic energy for three rotation levels.

Downloaded 04 Sep 2013 to 198.125.229.230. This article is copyrighted as indicated in the abstract. Reuse of AIP content is subject to the terms at: http://pop.aip.org/about/rights_and_permissions

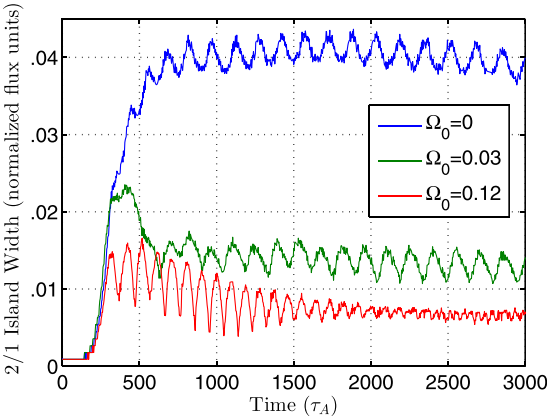

FIG. 10. Evolution of the $m/n = 2/1$ island width for three toroidal levels.

evolution of the (2,1) island width with three rotation levels. It is clear that plasma toroidal rotation can greatly reduce the island width even at a very low level of $\Omega_0/\omega_A = 0.03$. This result is consistent with shielding of magnetic islands due to differential rotation.[12–15] This result is also consistent with the NSTX experiment where the rotation shear was found to increase the threshold of NTM onset.[6] It should be pointed that the calculated island width depends somewhat on the value of resistivity used. Our simulation results indicate that the island width increases as resistivity increases. The scaling of island width with resistivity will be investigated and reported in a future publication.

Finally, we have examined the effects of NRK on rotation profile. Figure 11 compares the equilibrium rotation profile (red, t = 0) and the rotation profile in the saturated phase (blue, t = 3000). We observe that the NRK flattens the profile in the core. The amount of flattening is quite small. Thus, in this case, the NRK itself does not affect the rotation significantly.

V. DISCUSSIONS AND CONCLUSIONS

In this work, we have carried out a systematic study of linear and nonlinear evolution of the non-resonant internal kink mode in NSTX plasmas with and without rotation. The

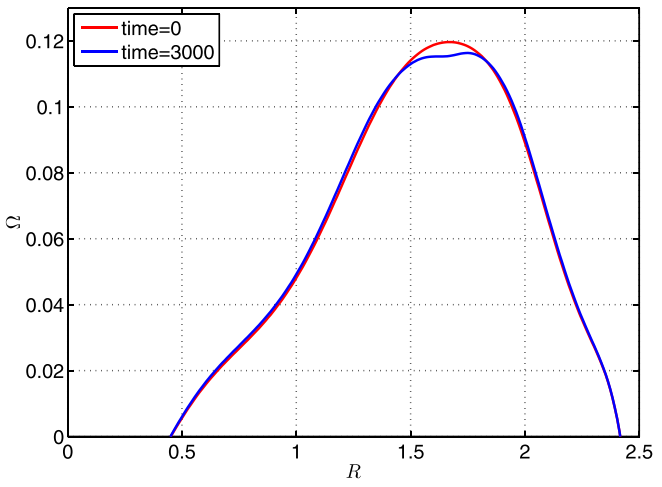

FIG. 11. Toroidal rotation profile at $t = 0$ and $t = 3000$.

work extends previous simulation studies[1] to finite plasma rotation. We find that a finite rotation, even at low levels, can greatly suppress the induced (2,1) island. We have also discovered an intriguing new dynamic nonlinear state at zero rotation. In this static case, a quasi-periodic phase was found after the initial mode saturation. In this new nonlinear regime, the magnetic topology oscillates between a helical state and a quasi-axisymmetric state. The mechanism and implication of this new nonlinear oscillation will be the subject of future work.

The results of our simulations were based on the parameters and profiles of an NSTX plasma (shot # 124379 at $t = 0.635$ s) where soft X-ray (SXR) data showed a saturated (2,1) mode of tearing parity together with a strong (1,1) component. This (2,1) mode is presumed to be an NTM with an island structure based on the inversion found in the SXR signal near the $q = 2$ surface. Our work was originally motivated by the previous work[1] which suggested that the induced (2,1) island by the non-resonant (1,1) mode can trigger the (2,1) NTM. Our results show, however, that the simulated (1,1) mode rotates at a mode frequency close to the core rotation frequency, whereas in the experiment the (1,1) was seen to rotate together with the (2,1) component at the $q = 2$ rotation frequency. Thus, the experimental (1,1) mode appears to be just a coupled component of the resistive (2,1) NTM rather than the simulated ideal non-resonant kink mode. This discrepancy may come from the lack of neoclassical effects in our simulation model. The neoclassical effects can also lead to significant damping of toroidal rotation due to the NRK. Nonetheless our results still indicate that the ideal non-resonant kink mode can provide a seed island (even at a rotationally reduced width) for the (2,1) NTM as long as it is excited when q_{min} is sufficiently close to unity. Interestingly our results of a saturated rotating NRK mode agree very well with the observed LLM in MAST where the LLM was identified to be an ideal non-resonant (1,1) kink mode with no sign of magnetic islands in the SXR signal. Our results are also similar to the recent numerical results of MAST equilibria with helical core under conditions of weak reversed central shear.[16,17]

In addition to lacking neoclassical effects, the results presented here were obtained without the important kinetic effects of energetic beam ions (although the beam-induced plasma rotation is included). Previous work has indicated that the fast beam ions can have a moderate stabilizing effect on the ideal kink mode.[1,3] Our initial simulations with beam ions show a large stabilizing effect at zero rotation. Future work will consider the effects of energetic beam ions on both linear stability and nonlinear saturation including the excitation of fishbone modes.

In conclusion, we have performed extensive nonlinear simulation of the non-resonant internal kink mode in NSTX plasmas with finite plasma toroidal rotation. The numerical results show that, at the experimental level, plasma rotation has little effect on either equilibrium or linear stability. However, rotation has significant effects on the nonlinear dynamics of the (1,1) mode evolution and the induced (2,1) island. The simulation results show that, at finite rotation, a rotating helical equilibrium is maintained in the nonlinear

Downloaded 04 Sep 2013 to 198.125.229.230. This article is copyrighted as indicated in the abstract. Reuse of AIP content is subject to the terms at: http://pop.aip.org/about/rights_and_permissions

phase. In contrast, for non-rotating cases, the nonlinear evolution exhibits dynamic oscillation between a quasi-2D state and a helical state with corresponding oscillation in the mode kinetic energy. Furthermore, the effects of sheared rotation are found to greatly suppress the (2,1) magnetic island even at a low level. These results have important implications for confinement of both thermal plasma and energetic particles in spherical and conventional tokamaks. First, the plasma rotation could be used to control NTM, by reducing its seed island. Second, the obtained rotating helical state could lead to large energetic particle transport and broadening of the current profile. The role of energetic particles on this kink mode will be the subject of a future publication.

ACKNOWLEDGMENTS

The authors are grateful to Dr. Wonchull Park, Dr. Deyong Liu, Dr. Huishan Cai, and Mr. Wei Shen for helpful discussions. One of the authors (G. Y. Fu) thanks Dr. Stefan Gerhardt and Dr. Steve Jardin for information about the NSTX plasma profiles used in this work. This work was supported by the US Department of Energy under DE-AC02-09CH11466, and NMCSFP under Contract Nos. 2013GB107003 and 2013GB111001. The simulations were carried out using the supercomputer Hopper at NERSC.

[1]J. Breslau, M. Chance, J. Chen, G. Fu, S. Gerhardt, N. Gorelenkov, S. Jardin, and J. Manickam, Nucl. Fusion **51**, 063027 (2011).
[2]R. J. Hastie, T. C. Hender, B. A. Carreras, L. A. Charlton, and J. A. Holmes, Phys. Fluids **30**, 1756 (1987).
[3]I. Chapman, M.-D. Hua, S. Pinches, R. Akers, A. Field, J. Graves, R. Hastie, and C. Michael, Nucl. Fusion **50**, 045007 (2010).
[4]M.-D. Hua, I. T. Chapman, S. D. Pinches, R. J. Hastie, and T. M. Team, EPL **90**, 55001 (2010).
[5]J. Manickam, N. Pomphrey, and A. Todd, Nucl. Fusion **27**, 1461 (1987).
[6]S. Gerhardt, D. Brennan, R. Buttery, R. La Haye, S. Sabbagh, E. Strait, M. Bell, R. Bell, E. Fredrickson, D. Gates, B. LeBlanc, J. Menard, D. Stutman, K. Tritz, and H. Yuh, Nucl. Fusion **49**, 032003 (2009).
[7]J. Menard, R. Bell, D. Gates, S. Kaye, B. LeBlanc, F. Levinton, S. Medley, S. Sabbagh, D. Stutman, K. Tritz, and H. Yuh: Phys. Rev. Lett. **97**, 095002 (2006).
[8]S. Gerhardt, D. Gates, S. Kaye, R. Maingi, J. Menard, S. Sabbagh, V. Soukhanovskii, M. Bell, R. Bell, J. Canik, E. Fredrickson, R. Kaita, E. Kolemen, H. Kugel, B. Le Blanc, D. Mastrovito, D. Mueller, and H. Yuh, Nucl. Fusion **51**, 073031 (2011).
[9]W. Park, E. V. Belova, G. Y. Fu, X. Z. Tang, H. R. Strauss, and L. E. Sugiyama, Phys. Plasmas **6**, 1796 (1999).
[10]B. van der Holst, Phys. Plasmas **7**, 4208 (2000).
[11]C. Wahlberg and A. Bondeson, Phys. Plasmas **7**, 923 (2000).
[12]R. Fitzpatrick, Nucl. Fusion **33**, 1049 (1993).
[13]X. Wang and A. Bhattacharjee, Phys. Plasmas **4**, 748 (1997).
[14]C. C. Hegna, J. D. Callen, and R. J. LaHaye, Phys. Plasmas **6**, 130 (1999).
[15]Q. Yu, S. Günter, K. Lackner, and M. Maraschek, Nucl. Fusion **52**, 063020 (2012).
[16]W. A. Cooper, J. P. Graves, A. Pochelon, O. Sauter, and L. Villard, Phys. Rev. Lett. **105**, 035003 (2010).
[17]W. A. Cooper, J. P. Graves, O. Sauter, I. T. Chapman, M. Gobbin, L. Marrelli, P. Martin, I. Predebon, and D. Terranova, Plasma Phys. Controlled Nucl. Fusion Res. **53**, 074008 (2011).

Downloaded 04 Sep 2013 to 198.125.229.230. This article is copyrighted as indicated in the abstract. Reuse of AIP content is subject to the terms at: http://pop.aip.org/about/rights_and_permissions